BAMS Article

Megaflashes

Just How Long Can a Lightning Discharge Get?

Walter A. Lyons, Eric C. Bruning, Tom A. Warner, Donald R. MacGorman, Samantha Edgington, Clemens Tillier, and Janusz Mlynarczyk

ABSTRACT: The existence of mesoscale lightning discharges on the order of 100 km in length has been known since the radar-based findings of Ligda in the mid-1950s. However, it took the discovery of sprites in 1989 to direct significant attention to horizontally extensive "megaflashes" within mesoscale convective systems (MCSs). More recently, 3D Lightning Mapping Arrays (LMAs) have documented sprite-initiating lightning discharges traversing several hundred kilometers. One such event in a 2007 Oklahoma MCS having an LMA-derived length of 321 km, has been certified by the WMO as the longest officially documented lightning flash. The new Geostationary Lightning Mapper (GLM) sensor on *GOES-16/17* now provides an additional tool suited to investigating mesoscale lightning. On 22 October 2017, a quasi-linear convective system moved through the central United States. At 0513 UTC, the GLM indicated a lightning discharge originated in northern Texas, propagated north-northeast across Oklahoma, fortuitously traversed the Oklahoma LMA (OKLMA), and finally terminated in southeastern Kansas. This event is explored using the OKLMA, the National Lightning Detection Network (NLDN), and the GLM. The NLDN reported 17 positive cloud-to-ground flashes (+CGs), 23 negative CGs (−CGs), and 37 intracloud flashes (ICs) associated with this massive discharge, including two +CGs capable of inducing sprites, with others triggering upward lightning from tall towers. Combining all available data confirms the megaflash, which illuminated 67,845 km^2, was at least 500 km long, greatly exceeding the current official record flash length. Yet even these values are being superseded as GLM data are further explored, revealing that such vast discharges may not be all that uncommon.

AFFILIATIONS: **Lyons**—FMA Research, Fort Collins, Colorado; **Bruning**—Texas Tech University, Lubbock, Texas; **Warner**—ZT Research, Rapid City, South Dakota; **MacGorman**—NOAA/National Severe Storms Laboratory/Warning Research and Development Division, Norman, Oklahoma; **Edgington, Tillier**—LMATC, Lockheed Martin, Palo Alto, California; **Mlynarczyk**—AGH University of Science and Technology, Krakow, Poland

https://doi.org/10.1175/BAMS-D-19-0033.1
Corresponding author: Walter A. Lyons, walyons@frii.com
Supplemental material: https://doi.org/10.1175/BAMS-D-19-0033.2
In final form 9 October 2019

Lightning is sometimes casually described as "a really big spark." According to the Glossary of Meteorology (American Meteorological Society 2015), a lightning flash is a transient, high-current electric discharge with pathlengths measured in kilometers. Even "ordinary" lightning is impressive, but like most geophysical phenomena, the metrics that quantify its properties span broad ranges, with values at the extreme ends of the distributions being hard both to observe and quantify.

So how "big" can a lightning flash actually get? The length in the vertical dimension is generally limited by the altitude of the main charge centers in the cloud (typically 6–10 km) and certainly by the cloud top, rarely more than ~20 km high. The horizontal extent of a flash within the cloud, however, can be much longer, reaching "mesoscale" dimensions in large storm systems, although this terminology lacks precision. As Orlanski (1975) noted, various definitions of mesoscale range from 4 to 400 km. For our purposes here, we will elect a threshold of 100 km for flashes we consider mesoscale, and these are the focus of this paper.

The first hint of lightning with mesoscale dimensions was gleaned from the fast-scanning radar studies of Ligda (1956). Some lightning channels, in what today would be termed a leading-line trailing-stratiform (LLTS) mesoscale convective system (MCS), originated from the upper level of the storm's leading edge and propagated rearward down into the light precipitation zone by as much as 160 km. These reports remained mostly a curiosity for several decades until the realization that lightning routinely occurred in the stratiform region of storm systems (Mazur and Rust 1983; Rutledge and MacGorman 1988; Mazur et al. 1998). Interest in the spatial extent of cloud flashes developed further in response to issues involving aviation and range safety (Pitts et al. 1988; Mazur 1989), atmospheric chemistry (Barth et al. 2015), the interpretation of cloud-top optical emissions for total lightning measurements by satellite sensors (Vonnegut et al. 1985), and the discovery of red sprites in 1989 (Franz et al. 1990; Lyons and Williams 1994; Williams 1998).

Total lightning refers to the sum of flashes that strike ground [cloud-to-ground flashes (CGs)] and flashes that do not [intracloud flashes (ICs)]. CGs can have one or more discrete, large current surges to ground (each called a return stroke), traveling through the same or sometimes separate channels. CG impacts dominate concerns regarding public safety, electric power grids, and the initiation of wildfires. A CG can lower either negative charge to ground (–CG; constituting roughly 90% of CGs on average, though this value is highly variable) or positive charge (+CG). Modern, ground-based lightning detection networks, such as the U.S. National Lightning Detection Network (NLDN), locate 80%–95% of CG ground strikes with an average accuracy better than 500 m (Cummins et al. 1998; Cummins and Murphy 2009). ICs have historically received less attention, even though they constitute perhaps three quarters of all lightning discharges. This value is also highly variable from region to region and storm to storm and even during a single storm (Boccippio et al. 2001; Rakov and Uman 2007). A satellite-borne sensor that responds to the optical energy emerging from cloud tops, such as that providing the data examined later in this paper, detects total lightning.

Besides being intrinsically interesting as extreme events, exceptionally long lightning discharges propagating through the stratiform precipitation region of an MCS sometimes produce exceptionally powerful +CGs, which in turn induce a number of unusual phenomena, including sprites (Franz et al. 1990). Such exceptional CGs result from propagating lightning channels tapping into huge reservoirs of positive charge present within the MCS stratiform region (Marshall and Rust 1993; Stolzenburg et al. 1998; Williams 1998; Carey et al. 2005; Lyons et al. 2009; Williams et al. 2010). A frequent scenario involves a lightning discharge originating near the top of the convective cells in the leading line (~8–10 km altitude) and then traveling rearward and downward, following the trajectory of descending positively charged ice crystals, often to near the melting layer (Carey et al. 2005; Ely et al. 2008; MacGorman et al. 2008; Lang et al. 2010). The discharge leaders then can continue at that approximate altitude while

generating multiple CGs often separated by tens of kilometers. Some of the +CGs can result in lightning-triggered upward lightning (LTUL) from tall towers and wind turbines (Warner et al. 2012, 2013, 2018), while others may lower sufficient charge to ground to induce sprites (Lyons et al. 2009; Lang et al. 2010) and may, on occasion, do both (Lyons et al. 2012, 2014).

Sprites are vast (on the scale of thousands of cubic kilometers), but brief (<~100 ms), faintly glowing discharges originating around 70–75 km altitude that first extend downward and then upward through the middle atmosphere (Lyons et al. 2009). They are induced by highly atypical CGs (almost always a +CG), most commonly found in MCS stratiform regions, that lower exceptional amounts of positive charge (up to several hundred coulombs) to the ground (Boccippio et al. 1995; Lyons et al. 2003; Williams et al. 2010). The parameter that determines whether a +CG becomes a sprite parent (SP+CG) is the charge moment change (CMC), defined as the product of the vertical lightning channel length and the amount of charge lowered to ground (Cummer at al. 2013; Huang et al. 1999; Lyons 2006). For SP+CGs, the CMC magnitude results not just from the charge lowered by the high current return stroke, but also includes what is usually a much larger contribution from a lower amperage continuing current flowing to ground over an extended time period following the return stroke. This is a consequence of lightning channels inside the cloud continuing to intercept horizontally extensive positive charge pools within one or more layers as they propagate deeper and deeper into the stratiform region (Lang et al. 2010).

Early evidence that multiple SP+CGs could be produced by a single mesoscale flash came from a low-light video camera network. The triangulated locations of seven sequential "dancing sprites," within an 800 ms time window, translated west to east above an MCS trailing stratiform region and synchronized with the +CGs in the storm cloud below (Armstrong and Lyons 2000). It seemed reasonable to assume that a single discharge dropping multiple +CGs over a distance of about 200 km was involved. The advent of 3D Lightning Mapping Array (LMA) systems (Thomas et al. 2004) confirmed that lightning discharges exceeding 100 km in length and spawning multiple CGs, of both polarities, often separated by considerable distances, were not uncommon (Lyons 2006). Until recently, however, little attention has been paid to the maximum horizontal extent that could be attained by these mesoscale lightning discharges.

A world record lightning flash

A 2007 research campaign utilizing a low-light camera network, the NLDN, satellite, radar, and the Oklahoma LMA (OKLMA) (MacGorman et al. 2008) investigated sprites and especially their parent lightning within large nocturnal MCSs, including that on 20 June 2007, which produced almost 250 observed sprites (Lang et al. 2010). As noted by Lyons et al. (2009), numerous horizontally extensive lightning flashes occurred, including one selected for detailed analysis that produced 13 CGs, including two SP+CGs, while meandering from the leading line convection back through the trailing stratiform for "approximately 300 km." A decade later the World Meteorological Organization (WMO), in a review of extreme lightning events, proposed a methodology to use the OKLMA VHF source data to confirm the breadth of this flash, which extended a straight-line distance from the initiation to termination points for a total of 321 km over a period of 5.70 s (Lang et al. 2017). While not selected as part of a systematic search of LMA records, this event stands today as the *official* record for the longest distance for a continuous lightning discharge, even though it may not even have been the longest discharge in that particular MCS. (A flash lasting 7.74 s within a French MCS was the longest duration event officially verified in the WMO study.) But can a single lightning discharge travel even greater distances if the meteorological environment is favorable? Although the current official record length approaches the limit of what can be observed by any existing LMA, the Geostationary Lightning Mapper (GLM) on the new-generation GOES satellites is capable of detecting much larger flashes.

A new view from the Geostationary Lightning Mapper

Observing lightning from space has a long history. Early Defense Department spacecraft such as Vela (Turman 1977) and DMSP (Orville and Spencer 1979) revealed lightning patterns on continental and global scales. Film and low-light video cameras aboard the space shuttle in the Mesoscale Lightning Experiment characterized optical emissions from lightning, and also captured some of the first observations of sprites and elves (Vonnegut et al. 1985; Lyons and Williams 1994). From 1995 to 2000, the Optical Transient Detector (OTD) (Boccippio et al. 2000) and, from 1997 through 2015, the Lightning Imaging Sensor (LIS) on the TRMM satellite (Kummerow et al. 1998), mapped total lightning from low-Earth orbit and improved our understanding of the cloud-top radiances produced by discharges within the cloud (Peterson and Liu 2013). These programs all paved the way for the first GLM launched on 19 November 2016 on the (now) *GOES-16* satellite (Goodman et al. 2013). The GLM covers the Americas between 54°N/S, sampling changes in cloud-top optical radiances every 2 ms into pixels of ~8 km near the nadir to ~14 km at the highest latitudes (Rudlosky et al. 2019). Using a near-infrared 1 nm wide spectral band at 777.4 nm, the estimated GLM daytime lightning detection efficiency is around 70%, increasing to about 90% at night, with about a half-pixel locational accuracy. The research community is actively working to understand the strengths and limitations of this new resource, but it is clear that monitoring total lightning with high spatial and temporal resolution on a nearly hemispheric scale will yield a plethora of new insights (Rudlosky et al. 2019), including from studies of mesoscale lightning discharges and their impacts.

"Big" lightning in a quasi-linear convective system

The postlaunch GLM sensor's validation activities soon yielded a significant demonstration of its ability to map mesoscale lightning over the life cycle of an MCS in the central United States. At 1200 UTC 21 October 2017, a 500 hPa trough extended from eastern Montana south into New Mexico, ahead of which was found a sharp cold frontal boundary steadily moving east and south (see supplemental Figs. ES1 and ES2; https://doi.org/10.1175/BAMS-D-19-0033.2). By 1800 UTC, isolated cellular convection commenced ahead of the front, which then gradually evolved into what in older parlance would be termed a squall line, and is now more properly termed a quasi-linear convective system (QLCS). By 2100 UTC, the QLCS extended from Minnesota into northern Texas, with tornado watches issued for western Oklahoma and severe thunderstorm watches for eastern Kansas and northwestern Missouri. Severe weather reports included several tornadoes and large hail in western Oklahoma. After 0000 UTC 22 October, as it was approaching Oklahoma City (OKC), the continuous line developed a rapidly expanding trailing stratiform region with an embedded secondary precipitation maximum on radar. The trailing stratiform region reached its maximum areal coverage and reflectivity intensity during the 0400–0900 UTC time period, after which it decayed slowly through the dawn hours over Missouri and Arkansas.

Serendipitously, on this night several high-speed video camera systems had been deployed to monitor LTUL events from a cluster of tall TV broadcast towers northeast of OKC (Warner et al. 2013, 2018). Between 0217 and 0409 UTC, as the secondary precipitation maximum passed overhead, 39 LTUL events (each associated with a +CG striking within several tens of kilometers of the towers) were confirmed, along with vivid spider lightning displays.

It has been documented that some +CG lightning flashes in the trailing stratiform region that are favorable for producing LTULs can also induce sprites (Lyons et al. 2014; Warner et al. 2018). While no dedicated sprite-monitoring cameras were operational at this time, fortunately, an all-sky meteor-tracking camera located in Lamy, New Mexico, did capture sprites at 0431, 0438, 0450, and 0620 UTC. Although much of the stratiform region was beyond the range of the all-sky camera, we note the storm passed through the southern portion of the central plains region with the highest U.S. climatological probability of sprite-class lightning

production (Beavis et al. 2014). Based upon two decades of sprite forecasting experience, we are confident that the four optically confirmed sprites were only a small fraction of the total number. Typically, a total CMC value >500 C km (Huang et al. 1999; Qin et al. 2012), calculated over the duration of a +CG stroke and any subsequent continuing current, indicates a high probability of triggering a mesospheric electrical breakdown (i.e., a sprite). CMC measurements, however, are presently not routinely available, but the observed sprites suggest high CMC +CGs were indeed occurring in this storm, as discussed further below.

Lightning data from the NLDN were tabulated for the portion of the QLCS south of the Iowa–Missouri border (40.5°N) for its entire lifetime. From the QLCS's inception around 1800 UTC to its dissipation by 1200 UTC the next morning, the NLDN recorded 1,190,822 IC reports and 124,431 CG reports [as per the suggestion of Cummins and Murphy (2009), only records with ≥15 kA peak current magnitude were accepted as CGs for these statistics]. Of the CGs, 15.4% were +CGs. Flash rates for both CGs and ICs peaked between 0400 and 0600 UTC.

The availability of the new GLM sensor (Rudlosky et al. 2019) provided a different and highly revealing view of the QLCS electrical activity. An animated loop of GLM frames of this storm created for demonstration purposes (see Fig. ES3 in the supplemental material: https://doi.org/10.1175/BAMS-D-19-0033.2) makes it clear that, as the trailing stratiform developed after about 0100 UTC, there were really two spatially distinct lightning regimes. Large numbers of relatively small flashes repeatedly peppered the leading line cellular convection, while mesoscale dendritic lightning flashes periodically originated near the convective cores and propagated back into the expansive trailing stratiform region. As the night progressed, these massive discharges gradually became less frequent, but also larger (a behavior reminiscent of sprites commonly noted by researchers viewing low-light television displays over similar meteorological regimes).

One of the larger horizontally extensive flash sequences, when integrated over a 7.18 s interval, prompted further exploration, given that it crossed over part of the OKLMA (Fig. 1). The animated version of Fig. 1 (Fig. ES4 in the supplemental material: https://doi.org/10.1175/BAMS-D-19-0033.2) shows the popcorn-like, leading line lightning activity in southeastern Oklahoma and north Texas, while at 0513:27.500 UTC, an apparently continuous flash started in north Texas just south of the Red River and propagated north-northeastward into Kansas. The coincident radar reflectivity mosaic combined with NLDN reports (Fig. 2) shows the flash began close to the leading

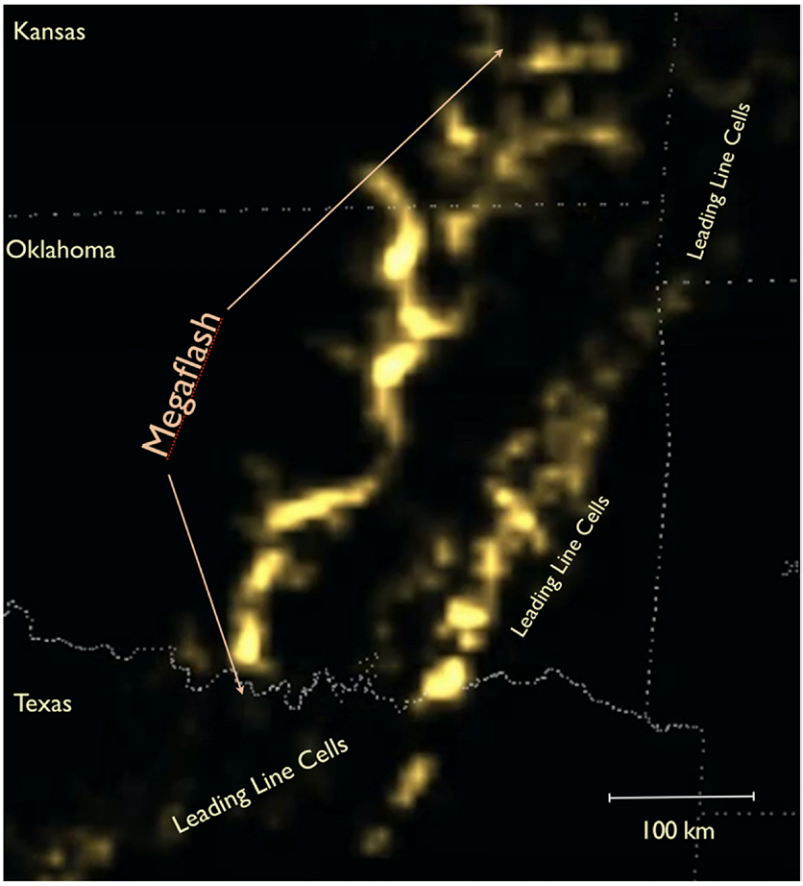

Fig. 1. Time integrated GLM radiances over 7.18 s beginning at 0513:27.433 UTC 22 Oct 2017. Two distinct electrical regimes are evident. The first is the cluster of smaller flashes in the leading line of convective cells stretching from eastern Oklahoma and then southwest into north Texas. The second regime is an extensive horizontal flash propagating from near the Red River in Texas across central Oklahoma into southeastern Kansas. An animated version of the larger QLCS (Fig. ES3) and of this figure (Fig. ES4) are included as electronic supplements.

line convection in northern Texas and then traversed the extensive secondary precipitation maximum of the trailing stratiform. The initial estimate of the GLM image flash length indicated it extended ~550 km end to end. Clearly this "megaflash," as we propose to call it, appears to greatly exceed the current official WMO distance record. Can we support the contention, with independent data, that the GLM mapped a single flash rather than an amalgam of smaller flashes, while also establishing the potential of the GLM to create a systematic census of megaflash characteristics over its coverage area?

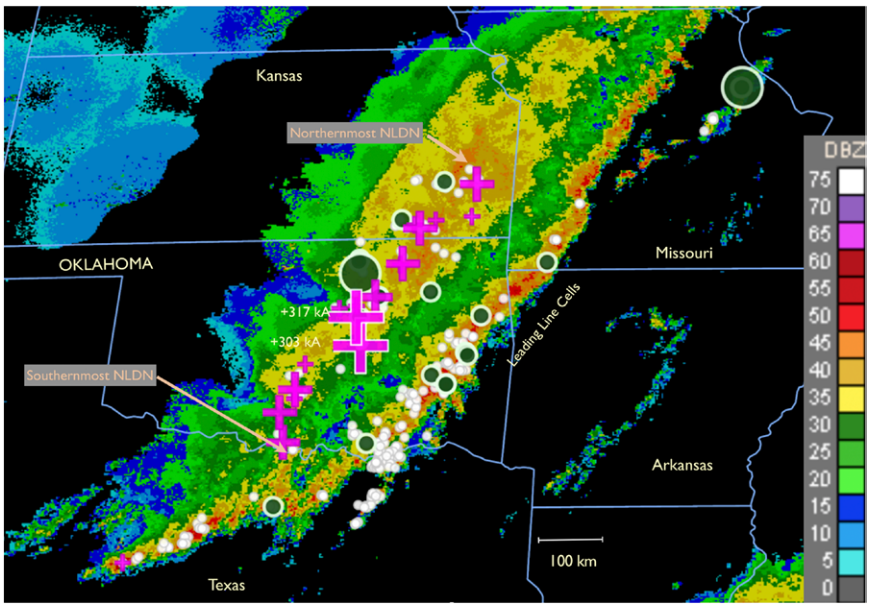

Fig. 2. NEXRAD base (0.5°) radar reflectivity mosaic at 0510–0515 UTC 22 Oct 2017, showing the QLCS portion extending from Missouri to Texas, which was moving steadily east and south. NLDN data for 6.52 s period south of 40.5°N (Missouri–Iowa border) encompass the megaflash (IC = white dots; –CG = green circles; +CG = magenta plusses; CG peak currents >75 kA use larger symbols and >300 kA largest pluses). The southern–and northernmost–NLDN reports indicated.

Documenting a megaflash

The NLDN and LMA provide two independent datasets suitable for demonstrating that the megaflash was a single lightning entity. Since it propagated through the eastern portion of the OKLMA (MacGorman et al. 2008), we will employ, in part, the WMO methodology used to evaluate the 2007 official record event (Lang et al. 2017). The location accuracy and detection efficiency of the OKLMA are analyzed in Chmielewski and Bruning (2016) and Weiss et al. (2018). The range of the system for mapping the three-dimensional location of lightning is typically 125 km from the center of the network, and for mapping the detailed plan location of lightning it is not much more than 200 km. Although some VHF sources are detected at longer ranges, the decreasing detection efficiency, significantly increasing location errors, and rapidly increasing altitude of the line-of-sight horizon below which sources cannot be seen, all act together to severely limit what can be seen much beyond 200 km. While large segments of the megaflash were within 200 km of the OKLMA center, we shall show it appeared to continue northward beyond that range. Thus, our analysis also had to consider data from the NLDN to define the terminus of the flash.

Figure 3 shows both LMA VHF sources and NLDN events, color-coded to indicate elapsed time during a 7.5 s period encompassing the flash (an animation, Fig. ES5, is included in the supplemental material: https://doi.org/10.1175/BAMS-D-19-0033.2). In accordance with the WMO methodology, only sources detected by at least seven stations and with a χ^2 value of <5 (two measures of data quality) were considered. The WMO procedure defined the location of the flash initiation as the mean location of the first 10 VHF sources, which were computed. Note, however, that it is not uncommon to observe bidirectional channel propagation from the initial breakdown point, including for flashes ultimately resulting in sprites (van der Velde et al. 2014; Warner et al. 2018), as was the case here. Therefore, the farthest south VHF source from the initiation point was also determined.

Figure 3 and its animation show the flash begins in extreme northern Texas and propagates along a somewhat meandering and dendritic pathway to the north-northeast. After 3.28 s, the most northerly LMA VHF source is detected in south-central Kansas. Assuming a straight line

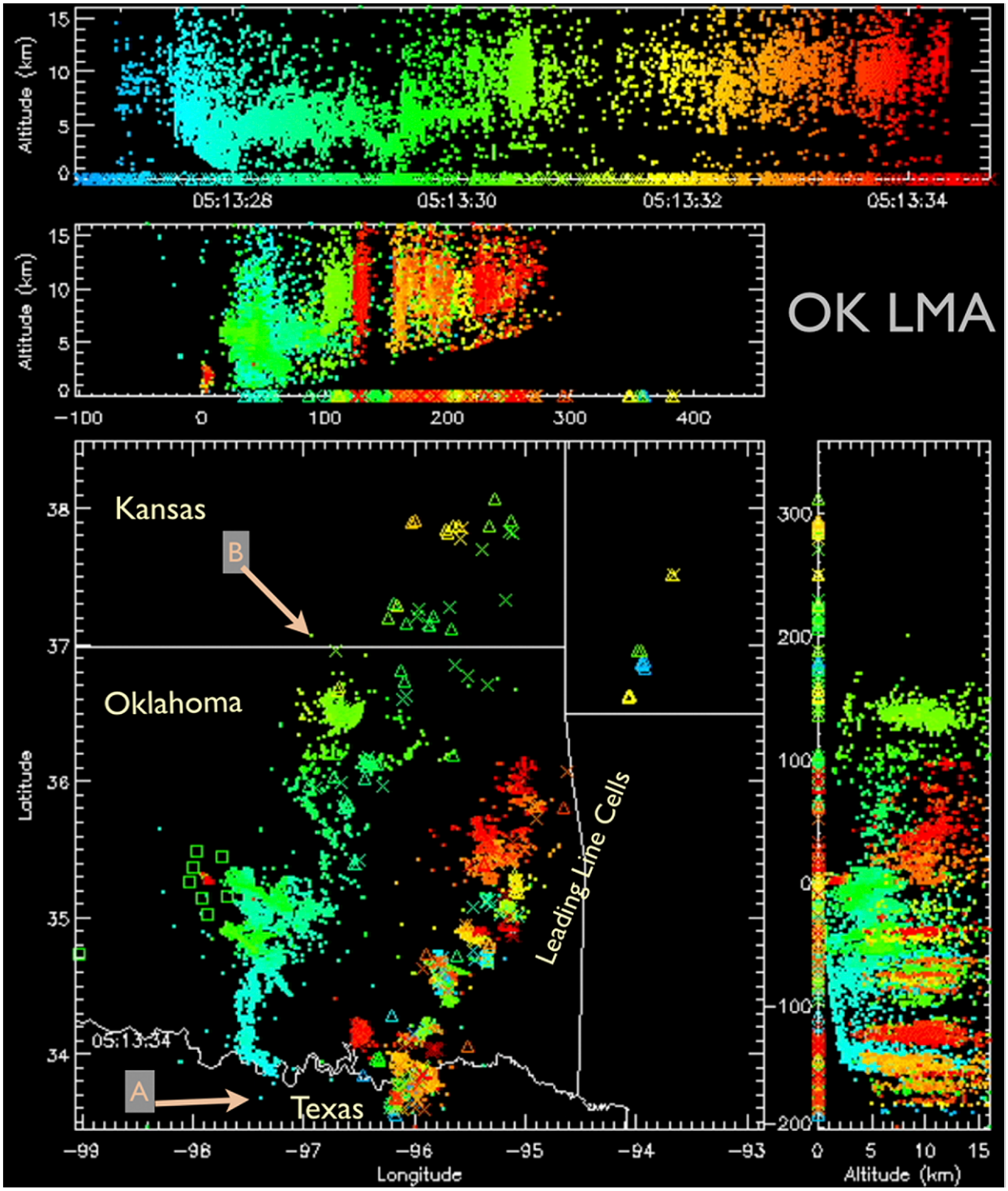

Fig. 3. Oklahoma LMA time color-coded plots for the 7.5 s period starting 0513:27.00 UTC 22 Oct 2017. Top panel is an altitude–time (*Z*–*T*) display, with the main panel being an *X*–*Y* plan view, along with *X*–*Z* and *Y*–*Z* plots above and to the right, respectively. NLDN reports over that time period, also time color-coded, shown as triangles (any negative events) or ×s (any positive events). LMA receivers located as green rectangles in Oklahoma. The "A" and "B" refer to the farthest south and north LMA sources, respectively, for the megaflash. An animation is included as an electronic supplement (Fig. ES5: see https://doi.org/10.1175/BAMS-D-19-0033.2).

propagation between start and finish implies a negative leader propagation speed through positive charge layers of ~1.1 × 10^5 m s^{-1}, which is consistent with prior observations (Bór et al. 2018; van der Velde et al. 2014). The LMA time–height display of the megaflash (Fig. 3) shows it begins around 8–9 km MSL, and over the next 500 ms descends into the trailing stratiform region to around 2–6 km MSL, and sometimes even lower, as it moves northward. It was likely occasionally visible as classic "spider lightning" (Mazur et al. 1998) near the base of the trailing stratiform region clouds (ceilings reported as varying between 1.5 and 2.8 km AGL, with lower scud below) as proposed by Williams (1998) and Warner et al. (2018). With NLDN reports continuing along the GLM illuminated path well into southeastern Kansas, the megaflash clearly outruns the nominal ~200 km range for mapping the discharge plan location by the OKLMA, whose detection efficiency decreases and line-of-site horizon rises rapidly as the lightning channels extended from northeastern Oklahoma into Kansas.

A plot of 6.5 s of NLDN data starting at 0513:27.500 UTC illustrates the two distinct electrical regimes present (Fig. 4, and Fig. ES6, its animation in the supplemental material: https://doi.org/10.1175/BAMS-D-19-0033.2). (In this case, the ICs, –CGs and +CGs are plotted as reported by the NLDN, without reclassifying any CGs with peak currents <15 kA as ICs.) The NLDN animation shows the activity within the leading line convection as spatially and temporally random, and primarily composed of ICs and –CGs. The megaflash begins in the NLDN data at 0513:27.500 UTC, some 3 ms after the first LMA sources, just south of the Red River in Texas, as a reported 10.3 kA +CG followed 2 ms later by a reported +IC slightly farther south. Thereafter the activity marches northward, finally ending in southeast Kansas. The most northerly NLDN event from the megaflash was a reported –IC at 0513:30.459 UTC. (After a 109 ms delay, several more NLDN reports did occur south and west of the northern terminus. They may or may not have been part of the megaflash but, in any case, did not affect the flash distance estimate.) If traveling a straight line (i.e., ignoring any meandering) from the first NLDN report to the northernmost event, the negative leader speed was ~1.5 × 10^5 m s^{-1}, similar to that derived from the LMA. After reaching its northern terminus, sporadic pulses of lightning were detected by the NLDN, LMA, and GLM at points along the initial channel. Such rebrightening of segments within horizontally extensive channels is common (Warner et al. 2018; Bór et al. 2018), and has been noted in LIS reconstructions of large flashes (Peterson et al. 2017).

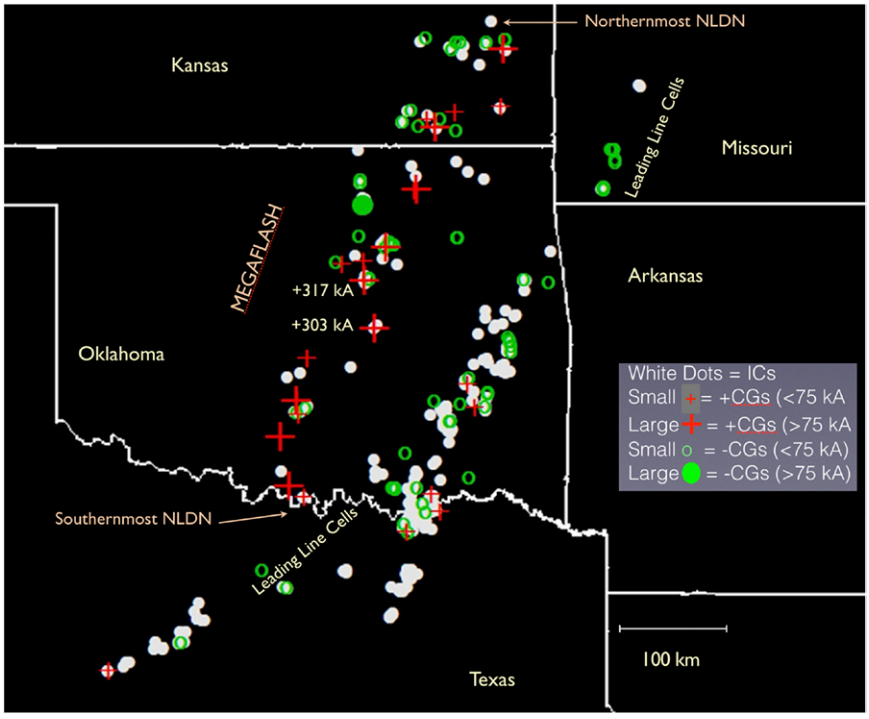

Fig. 4. NLDN reports (not adjusted for CGs < 15 kA) for 6.5 s period starting 0513:27.500 UTC 22 Oct 2017 showing the two electrical activity regimes: 1) the leading line convective cells, and 2) the massive megaflash in the trailing stratiform region in central Oklahoma and southeastern Kansas (IC = white dots; –CG = green circles; +CG = red pluses; +CG peak currents >75 kA enlarged). The two >300 kA +CGs with huge CMC values capable of inducing sprites are indicated. An animated version of this figure is included as an electronic supplement (Fig. ES6).

Along the path of the megaflash, the NLDN (uncorrected for the 15 kA peak current threshold) reported 37 ICs, 23 –CGs (including 10 LTULs), and 17 +CGs. There were 10 +CGs >75 kA (versus none in the leading

line cells). At ~2.4 s into the event, two +CGs of 303 kA and 317 kA occurred 42 ms apart as the megaflash propagated northeast of OKC. By chance, the extremely low-frequency (ELF) waveform signatures of both of these +CGs were recorded by a receiver in Patagonia (Mlynarczyk et al. 2017). Using these ELF data and standard techniques (Huang et al. 1999), the total computed charge moment changes were 3,140 and 3,600 C km, respectively, each almost certainly resulting in sprites.

Over the 18 h duration of the QLCS, −CGs with large peak currents [>75 kA, as defined by Lyons et al. (1998)] outnumbered their positive counterparts by 3.56 to one. In 13 of the 18 h the largest peak current magnitudes were from −CGs. (The extremes recorded by the NLDN were −448 kA and +362 kA.) In midlatitude MCSs, however, −CGs with large peak currents very rarely have CMC values exceeding the threshold for sprites (Qin et al. 2012; Lang et al. 2013). We note that after the onset of the trailing stratiform region around 0000 UTC, there was a distinct spatial sorting of large peak current CGs by polarity. Most of the large peak current −CGs occurred within the leading line cells, with the large majority of the large peak current +CGs being in the stratiform region. Between 0000 and 0600 UTC, 82% of the +CGs >75 kA were found in the trailing stratiform. Many of these powerful +CGs most likely also had large CMC values, typical for a region of the United States with a high density of sprite-class lightning from MCSs (Beavis et al. 2014; Lyons et al. 2009; Williams et al. 2010).

While this particular megaflash passed too far east of the OKC tower farm to initiate LTULs there, a 79 kA +CG striking close to a broadcast tower in Tulsa, Oklahoma, induced upward positive leaders that the NLDN reported as 10 −CGs and one −IC (all within 150 m of the tower) following the triggering +CG return stroke, consistent with previous LTUL studies (Warner et al. 2012). Also notable, in the seconds before and after and, sporadically during, the megaflash, the LMA detected periodic bursts of low-altitude and low-power VHF sources southwest of OKC near the center of the LMA domain. These sources correlated with the locations of individual wind turbines and appeared to be weak discharges emanating from rotating wind turbine blades similar to that reported by Montanyà et al. (2014). This suggests elevated electric field values near the surface may have been present on a regional scale within the trailing stratiform area.

Figure 5 and Fig. ES7 (its animation in the supplemental material: https://doi.org/10.1175/BAMS-D-19-0033.2) summarize the observations. The GLM presentation was derived from the operational level 2 (L2) files that provide geolocated events, groups, and flashes. The group or flash data were not used, however, as GLM events were renavigated to the GOES fixed grid coordinates, removing the assumed lightning emission height used to geolocate the GLM L2 data. The fixed grid coordinates align exactly with the GLM pixel orientation, but geolocate lightning where the view angle from the satellite intersects with Earth's surface. The shape of the events was restored (using a lookup table specified in fixed grid coordinates) and exploited the stable pointing of the *GOES-16* platform to identify those events that likely came from the same GLM detector pixel. This made it possible to produce the visualization in Fig. 5. The well-aligned, spatially extensive pixels were used to sum the data in order to produce the total optical energy received at each location. Thus, the GLM locations are offset horizontally somewhat from the mapped LMA and NLDN locations in Fig. 5 by parallax errors. These errors are identical to those inherent in data from the Advanced Baseline Imager (ABI) (Schmit et al. 2017). NLDN events plotted as ICs in Fig. 5 included both those it identified as ICs and those it classified as CGs whose peak current magnitudes were less than 15 kA. The remaining strokes were considered CGs. All LMA sources located between 0 and 20 km MSL altitude were retained as long as they were located by at least seven stations and had a χ^2 value of <5.0.

Just how long was this megaflash? Using the GLM, the maximum great circle distance between any two illuminated pixels was 547 km. The illuminated cloud area detected totaled 67,845 km^2 (the sum of the GLM grid square areas shown in Fig. 5), a measurement that includes some broadening of the optical footprint due to light scattering by the cloud. By combining the

WMO methodology, which uses only LMA data, with the NLDN reports, the great circle distances between candidate most-distant discharge elements are computed. Note this approach ignores the meandering nature of many large flashes, such as a semi-horseshoe-shaped flash in Kansas in 2013 with a path of ~175 km, but with end points only ~50 km apart (Lyons et al. 2014). For the 22 October 2017 megaflash, the northernmost terminus can be considered either 1) the farthest north LMA VHF source, *or* 2) the farthest north detection by the NLDN. The latter is clearly preferable as the lightning activity greatly exceeded the range of the OKLMA. For the southernmost, we can consider 1) the mean location of the first 10 LMA VHF sources, 2) the farthest south LMA source, 3) the first NLDN event, and 4) the farthest south NLDN event. Table 1 presents the matrix of results.

We deem it reasonable to use the farthest south LMA source and the farthest north NLDN event to define the path-length, which yields 524.2 km. No error bars are considered here, though we note a typical locational accuracy for the NLDN is ~250–500 m (Cummins and Murphy 2009). The LMA sources were nominally located with <800 m error near the initiation and northernmost detected VHF sources of the megaflash (Chmielewski and Bruning 2016; Weiss et al. 2018). Expected source detection efficiency (Chmielewski and Bruning 2016, their Fig. 6K) is about 60% at 200 km from the center of the OKLMA (for elevated sources), and about 70% near the flash origin. An empirical examination of the OKLMA data showed that any sources below 5 km MSL were not located beyond a 200 km range, so the

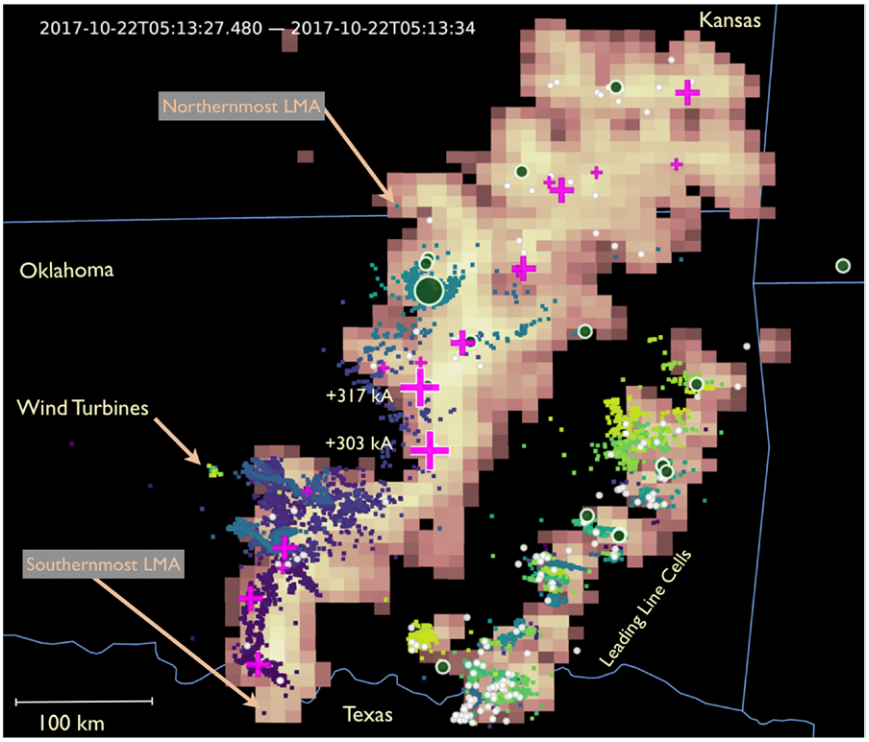

Fig. 5. Lightning observations over a 6.52 s period starting 0513:27.48 UTC 22 Oct 2017 in central and eastern Oklahoma (state borders, blue). For scale, each GLM pixel is separated by 9 km, GLM events (large rectangles) are colored by total energy during the observation interval at the GLM entrance aperture on a logarithmic scale between 10^{-15} (dark pink) and 10^{-11} J (yellow). NLDN observations (IC = white circles; –CG = green circles; –CG >75 kA use larger green circle; +CG = magenta pluses; +CG >75 kA use larger and >300 kA largest pluses). LMA events (small points) are colored by time (progressing from purple to dark cyan to light green to yellow). New GLM and NLDN detections occurred throughout the time interval, while the northernmost LMA source associated with the megaflash occurred at 0513:30.783 UTC in extreme southern Kansas. LMA observations continued after the megaflash within the cells in the leading convective line. An animated version is included as an electronic supplement (Fig. ES7).

Table 1. Options for computing the maximum end-to-end horizontal extent[a] of the megaflash in the trailing stratiform region of the 22 Oct 2017 quasi-linear convective system in the U.S. central plains.

	Farthest north LMA source 37.0634°N, 96.9233°W	Farthest north NLDN event 38.0646°N, 95.2678°W
First 10 LMA sources 33.8834°N, 97.3028°W	355.3 km	499.7 km
Farthest south LMA source 33.6723°N, 97.3828°W	379.4 km	524.2 km
First NLDN event 33.8829°N, 97.3037°W	355.3 km	499.7 km
Farthest south NLDN event 33.8824°N, 97.3090°W	355.4 km	500.0 km

[a] Great circle distance using Haversine method. No adjustments applied to consider locational errors.

sources in the leading line to the east of the megaflash had to have come from higher-altitude discharges. It is evident from Fig. 5 that within the megaflash the LMA detections in northern Oklahoma quickly fell off beyond 200 km, consistent with the 5–6 km maximum altitude of the well-located sources near the center of the OKLMA. The southernmost source was within 200 km, but was isolated ~20 km from the tight cluster of sources farther to the north near the Red River. While this could possibly be noise, with a χ^2 of 1.7, this seems unlikely. Being conservative, one might elect to ignore the southernmost LMA source and use the next one farther north (also with a χ^2 of ~1) yielding a distance of 508.7 km (not shown in Table 1). Regardless of which option is used (with a range spanning 355.3 to 524.2 km), this flash is *very* long.

Summary and discussion

This event was selected from a demonstration video of preoperational GLM visualizations primarily because it occurred partly within the OKLMA domain, thus permitting detailed analysis. The computed straight line start-to-end point distances depend on the data type elected: 1) 355–379 km utilizing only LMA VHF sources, 2) 500–524 km by combining LMA and NLDN reports, and 3) 547 km using the maximum breadth of the GLM illuminated pixels. While possibly not even the longest megaflash in the 21–22 October 2017 MCS, all measures for the 0513 UTC event easily exceed the current WMO's official longest distance flash record of 321 km established using only LMA VHF source data (Lang et al. 2017).

Depending on whether using the maximum horizontal extent determined by the NLDN, LMA or GLM, the duration of the megaflash was 4.85, 3.29, or 4.76 s, respectively, shorter than the two events reported in Lang et al. (2017).

Since this megaflash has not been evaluated by the WMO, it is not *officially* a new distance record. In any case, that exercise would be moot, as there may well have been even longer megaflashes in this particular QLCS, and likely have been in many other storm systems since. It was selected for detailed analysis based on the availability of independent data to support the contention that it was not merely an artifact due to a sequence of much smaller, but adjacent, flashes.

What constitutes a megaflash? It obviously is quantitatively longer than a "normal" flash, but lacking a climatological census of such events in the pre-GLM era, one cannot (yet) set a criterion based on, say, the upper one-tenth percentile of length. The flashes are clearly "mesoscale," although even here the terminology lacks precision. As discussed in the Introduction, we propose to use a length of 100 km as the lower limit for a megaflash. "Even" a 100 km discharge is certainly a "big" flash and, at an order of magnitude larger than a typical air mass thunderstorm, would span the distance between, say, the Chicago (O'Hare) and Milwaukee airports, or from Detroit to Toledo. But megaflashes may be qualitatively different in several key regards as well. It has long been noted by sprite researchers that only certain convective storm types produce significant numbers of sprites (Lyons 2006). The presence of numerous +CGs does not guarantee that even a few possess the large CMC values needed to induce sprites, such as in the case of supercells (Lyons et al. 2008). However, once an MCS develops a stratiform region of at least 10,000 km^2, the character of the stratiform lightning often changes (Lyons et al. 2003, 2009). Flashes longer than ~100 km in length (the square root of 10^4 km^2) appear to more readily tap into the vast positive charge reservoir(s) found in one or more layers within these stratiform regions. This allows the +CG continuing currents to lower massive amounts of positive charge to ground, with corresponding CMC values exceeding the threshold for sprites. We therefore propose a megaflash be defined as a continuous lightning flash with a horizontal pathlength of >100 km (not necessarily in a straight line) that may also produce one or more CGs of either polarity along its path, with some +CGs potentially having large CMCs and/or peak currents resulting in sprites and/or lightning-triggered upward lightning discharges (LTULs) from tall structures.

Megaflashes also pose a safety hazard, as they can be thought of as the stratiform region's version of the "bolt from the blue," sometimes occurring long after the local lightning threat appears to have ended. But some key questions remain: What is the population of megaflashes, and how long can they actually become?

With the GLM now operational, it appeared inevitable that megaflashes longer than this example would soon be found. And right on cue, a new paper by Peterson (2019) reports on a survey of GLM flashes throughout the Americas during calendar year 2018. Flashes with maximum group separations (lengths) of 582, 623, 659, 666, and 673 km, all within MCS stratiform regions, were revealed. Additionally, Peterson (2019) found a flash with a maximum illuminated area of 114,997 km^2, and one with an apparent duration of 13.496 s in another MCS.

All "records," official and otherwise, are meant to be broken. The WMO Commission of Climatology has recently empaneled an Ad-Hoc Evaluation Committee for the Assessment of Extreme Lightning Events. It will be tasked with reviewing, among other issues, the GLM-based determinations of extreme lightning. It should be noted that while GLM provides a remarkable new resource, its use is not without issues. Designed to operationally process lightning events on a hemispheric scale in real time, the algorithms can become bogged down during periods of intense activity. As discussed by Peterson (2019), "to overcome this, the algorithms quit when flashes become too complex, and this results in single natural lightning flashes being artificially split into multiple 'degraded' flashes." Therefore, hunting for megaflashes requires significant postprocessing of the raw GLM data, as performed by Peterson (2019). Determining the area of a flash from the cloud-top illumination also has some challenges. Developing a semi-objective methodology to derive lengths for meandering discharges is also far from straightforward. Regardless of the technical challenges, the field of atmospheric electricity has obtained a powerful new tool that, among other things, should be employed to better understand the exceptional discharges that induce many sprites and LTULs and also to develop a climatology of such megaflashes.

Where might the next "longest flash" be found for the WMO to certify? The 673 km event reported by Peterson (2019) occurred over southeastern Brazil, within a region known for some of the most powerful and expansive thunderstorms on Earth (Zipser et al. 2006). West African squall lines can likewise possess extensive stratiform regions (Williams et al. 2010), an area to be monitored by a GLM-like sensor on EUMETSAT's Meteosat Third Generation satellites starting in 2022. The central United States is home to QLCS "squall lines" spanning multiple states and huge mesoscale convective complexes (Maddox 1980), both known to produce large numbers of sprite-class lightning flashes (Beavis et al. 2014). A megaflash, once initiated, appears able to propagate almost indefinitely as long as adequate contiguous charge reservoirs exist in the secondary precipitation maxima of MCS stratiform regions. Is it possible that a future megaflash can attain a length of 1,000 km? We would not bet against that. Let the search begin.

Acknowledgments. We wish to thank Thomas Nelson (FMA Research) for processing the voluminous NLDN data files graciously provided by Vaisala, Inc. The assistance of Jessica Souza (University of Sao Paulo, Brazil/Texas Tech University) and Kristin Calhoun (Cooperative Institute for Mesoscale Meteorological Studies and NOAA/OAR/National Severe Storms Laboratory) are greatly appreciated. Valuable insights came through discussions with Earle Williams (Massachusetts Institute of Technology), Kenneth Cummins (The University of Arizona), Steven Cummer (Duke University), and Paul Krehbiel and Bill Rison (New Mexico Tech). Sprite observations were contributed by Thomas Ashcraft (Heliotown, New Mexico). Prior support for sprite research was provided to FMA Research, Inc., by DARPA (by the NIMBUS through a grant to Duke University). Partial support to Texas Tech University was provided through NASA Award NNX16AD24G (GLM validation) and NSF Award AGS-1352144 (CAREER Program). The radar mosaic was courtesy of Iowa State University/Iowa Environmental Mesonet (https://mesonet.agron.iastate.edu/docs/nexrad_composites/).

REFERENCES

American Meteorological Society, 2015: Lightning. Glossary of Meteorology, http://glossary.ametsoc.org/wiki/lightning.

Armstrong, R. A., and W. A. Lyons, 2000: Characterizing atmospheric electrodynamic emissions from lightning, sprites, jets and elves. Mission Research Corporation Final Rep., 212 pp.

Barth, M., and Coauthors, 2015: The Deep Convective Clouds and Chemistry (DC3) field campaign. *Bull. Amer. Meteor. Soc.*, **96**, 1281–1309, https://doi.org/10.1175/BAMS-D-13-00290.1.

Beavis, N. K., T. J. Lang, S. A. Rutledge, W. A. Lyons, and S. A. Cummer, 2014: Regional, seasonal, and diurnal variations of cloud-to-ground lightning with large impulse charge moment changes. *Mon. Wea. Rev.*, **142**, 3666–3682, https://doi.org/10.1175/MWR-D-14-00034.1.

Boccippio, D. J., E. R. Williams, S. J. Heckman, W. A. Lyons, I. T. Baker, and R. Boldi, 1995: Sprites, ELF transients, and positive ground strikes. *Science*, **269**, 1088–1091, https://doi.org/10.1126/science.269.5227.1088.

——, S. J. Goodman, and S. Heckman, 2000: Regional differences in tropical lightning distributions. *J. Appl. Meteor.*, **39**, 2231–2248, https://doi.org/10.1175/1520-0450(2001)040<2231:RDITLD>2.0.CO;2.

——, K. L. Cummins, H. J. Christian, and S. J. Goodman, 2001: Combined satellite- and surface-based estimation of the intracloud–cloud-to-ground lightning ratio over the continental United States. *Mon. Wea. Rev.*, **129**, 108–122, https://doi.org/10.1175/1520-0493(2001)129<0108:CSASBE>2.0.CO;2.

Bór, J., Z. Zelkó, T. Hegedüs, Z. Jäger, J. Mlynarczyk, M. Popek, and H. D. Betz, 2018: On the series of +CG lightning strokes in dancing sprite events. *J. Geophys. Res. Atmos.*, **123**, 11 020–11 047, https://doi.org/10.1029/2017JD028251.

Carey, L. D., M. J. Murphy, T. L. McCormick, and N. W. S. Demetriades, 2005: Lightning location relative to storm structure in a leading-line, trailing-stratiform mesoscale convective complex. *J. Geophys. Res.*, **110**, D03105, https://doi.org/10.1029/2003JD004371.

Chmielewski, V. C., and E. C. Bruning, 2016: Lightning mapping array flash detection performance with variable receiver thresholds. *J. Geophys. Res. Atmos.*, **121**, 8600–8614, https://doi.org/10.1002/2016JD025159.

Cummer, S. A., W. A. Lyons, and M. A. Stanley, 2013: Three years of lightning impulse charge moment change measurements in the United States. *J. Geophys. Res. Atmos.*, **108**, 5176–5189, https://doi.org/10.1002/jgrd.50442.

Cummins, K. L., and M. J. Murphy, 2009: An overview of lightning location systems: History, techniques and data uses with an in-depth look at the U.S. NLDN. *IEEE Trans. Electromagn. Compat.*, **51**, 499–518, https://doi.org/10.1109/TEMC.2009.2023450.

——, ——, E. A. Bardo, W. L. Hiscox, R. B. Pyle, and A. E. Pifer, 1998: A combined TOA/MDF technology upgrade of the U.S. National Lightning Detection Network. *J. Geophys. Res.*, **103**, 9035–9044, https://doi.org/10.1029/98JD00153.

Ely, B. L., R. E. Orville, L. D. Carey, and C. L. Hodapp, 2008: Evolution of the total lightning structure in a leading-line, trailing-stratiform mesoscale convective system over Houston, Texas. *J. Geophys. Res.*, **113**, D08114, https://doi.org/10.1029/2007JD008445.

Franz, R. C., R. J. Nemzek, and J. R. Winckler, 1990: Television image of a large upward electrical discharge above a thunderstorm system. *Science*, **249**, 48–51, https://doi.org/10.1126/science.249.4964.48.

Goodman, S. J., and Coauthors, 2013: The GOES-R Geostationary Lightning Mapper (GLM). *Atmos. Res.*, **125–126**, 34–49, https://doi.org/10.1016/j.atmosres.2013.01.006.

Huang, E., E. Williams, R. Boldi, S. Heckman, W. Lyons, M. Taylor, T. Nelson, and C. Wong, 1999: Criteria for sprites and elves based on Schumann resonance observations. *J. Geophys. Res.*, **104**, 16 943–16 964, https://doi.org/10.1029/1999JD900139.

Kummerow, C., W. Barnes, T. Kozu, J. Shiue, and J. Simpson, 1998: The Tropical Rainfall Measuring Mission (TRMM) sensor package. *J. Atmos. Oceanic Technol.*, **15**, 809–817, https://doi.org/10.1175/1520-0426(1998)015<0809:TTRMMT>2.0.CO;2.

Lang, T. J., W. A. Lyons, S. A. Rutledge, J. D. Meyer, D. R. MacGorman, and S. A. Cummer, 2010: Transient luminous events above two mesoscale convective systems: Storm structure and evolution. *J. Geophys. Res.*, **115**, A00E22, https://doi.org/10.1029/2009JA014500.

——, S. A. Cummer, S. A. Rutledge, and W. A. Lyons, 2013: The meteorology of negative cloud-to-ground lightning strokes with large charge moment changes: Implications for negative sprites. *J. Geophys. Res. Atmos.*, **118**, 7886–7896, https://doi.org/10.1002/jgrd.50595.

——, and Coauthors, 2017: WMO world record lightning extremes: Longest reported flash distance and longest reported flash duration. *Bull. Amer. Meteor. Soc.*, **98**, 1153–1168, https://doi.org/10.1175/BAMS-D-16-0061.1.

Ligda, M. G. H., 1956: The radar observation of lightning. *J. Atmos. Terr. Phys.*, **9**, 329–346, https://doi.org/10.1016/0021-9169(56)90152-0.

Lyons, W. A., 2006: The meteorology of transient luminous events—An introduction and overview. *Sprites, Elves and Intense Lightning Discharges*, M. Füllekrug, E. A. Mareev, and M. J. Rycroft, Eds., NATO Science Series II, Vol. 225, Springer, 19–56.

——, and E. R. Williams, 1994: Some characteristics of cloud-to-stratosphere "lightning" and considerations for its detection. *Proc. Symp. on the Global Electrical Circuit, Global Change and the Meteorological Applications of Lightning Information*, Nashville, TN, Amer. Meteor. Soc., 360–367.

——, M. Uliasz, and T. E. Nelson, 1998: Large peak current cloud-to-ground lightning flashes during the summer months in the contiguous United States. *Mon. Wea. Rev.*, **126**, 2217–2233, https://doi.org/10.1175/1520-0493(1998)126<2217:LPCCTG>2.0.CO;2.

——, E. R. Williams, S. A. Cummer, and M. A. Stanley, 2003: Characteristics of sprite-producing positive cloud-to-ground lightning during the 19 July 2000 STEPS mesoscale convective systems. *Mon. Wea. Rev.*, **131**, 2417–2427, https://doi.org/10.1175/1520-0493(2003)131<2417:COSPCL>2.0.CO;2.

——, S. A. Cummer, M. A. Stanley, K. Wiens, and T. E. Nelson, 2008: Supercells and sprites. *Bull. Amer. Meteor. Soc.*, **89**, 1165–1174, https://doi.org/10.1175/2008BAMS2439.1.

——, M. A. Stanley, J. D. Meyer, T. E. Nelson, S. A. Rutledge, T. J. Lang, and S. A. Cummer, 2009: The meteorological and electrical structure of TLE-producing convective storms. *Lightning: Principles, Instruments and Applications*, H. D. Betz et al., Eds., Springer Science Business Media, 389–417, https://doi.org/10.1007/978-1-4020-9079-017 1.

——, and Coauthors, 2012: Different strokes: Researching the unusual lightning discharges associated with sprites and jets and atypical meteorological regimes. *22rd Int. Lightning Detection Conf./4th Int. Lightning Meteorology Conf.*, Broomfield, CO, Vaisala, www.vaisala.com/sites/default/files/documents/Different%20Strokes%20Researching%20the%20Unusual%20Lightning%20Discharges%20Associated%20with.pdf.

——, and Coauthors, 2014: Meteorological aspects of two modes of lightning-triggered upward lightning (LTUL) events in sprite-producing MCS. *23rd Int. Lightning Detection Conf./5th Int. Lightning Meteorology Conf.*, Tucson, AZ, Vaisala, www.vaisala.com/sites/default/files/documents/Lyons%20et%20al-Meteorological%20Aspects%20of%20Two%20Modes%20of%20LTUL-2014-ILDC-ILMC.pdf.

MacGorman, D. R., and Coauthors, 2008: TELEX: The Thunderstorm Electrification and Lightning Experiment. *Bull. Amer. Meteor. Soc.*, **89**, 997–1013, https://doi.org/10.1175/2007BAMS2352.1.

Maddox, R. A., 1980: Mesoscale convective complexes. *Bull. Amer. Meteor. Soc.*, **61**, 1374–1387, https://doi.org/10.1175/1520-0477(1980)061<1374:MCC>2.0.CO;2.

Marshall, T. C., and W. D. Rust, 1993: Two types of vertical electrical structures in stratiform precipitation regions of mesoscale convective systems. *Bull. Amer. Meteor. Soc.*, **74**, 2159–2170, https://doi.org/10.1175/1520-0477(1993)074<2159:TTOVES>2.0.CO;2.

Mazur, V., 1989: A physical model of lightning initiation on aircraft in thunderstorms. *J. Geophys. Res.*, **94**, 3326–3340, https://doi.org/10.1029/JD094iD03p03326.

——, and W. D. Rust, 1983: Lightning propagation and flash density in squall lines as determined with radar. *J. Geophys. Res.*, **88**, 1495–1502, https://doi.org/10.1029/JC088iC02p01495.

——, X.-M. Shao, and P. R. Krehbiel, 1998: "Spider" lightning in intracloud and positive cloud-to-ground flashes. *J. Geophys. Res.*, **103**, 19811–19822, https://doi.org/10.1029/98JD02003.

Mlynarczyk, J., A. Kulak, and J. Salvador, 2017: The accuracy of radio direction finding in the extremely low frequency range. *Radio Sci.*, **52**, 1245–1252, https://doi.org/10.1002/2017RS006370.

Montanyà, J., O. van der Velde, and E. R. Williams, 2014: Lightning discharges produced by wind turbines. *J. Geophys. Res. Atmos.*, **119**, 1455–1462, https://doi.org/10.1002/2013JD020225.

Orlanski, I., 1975: A rational subdivision of scales for atmospheric processes. *Bull. Amer. Meteor. Soc.*, **56**, 527–530, https://doi.org/10.1175/1520-0477-56.5.527.

Orville, R. E., and D. W. Spencer, 1979: Global lightning flash frequency. *Mon. Wea. Rev.*, **107**, 934–943, https://doi.org/10.1175/1520-0493(1979)107<0934:GLFF>2.0.CO;2.

Peterson, M., 2019: Research applications for the Geostationary Lightning Mapper (GLM) operational lightning flash data product. *J. Geophys. Res. Atmos.*, **124**, 10205–10231, https://doi.org/10.1029/2019JD031054.

——, and C. Liu, 2013: Characteristics of lightning flashes with exceptional illuminated areas, durations, and optical powers and surrounding storm properties in the tropics and inner subtropics. *J. Geophys. Res. Atmos.*, **118**, 11727–11740, https://doi.org/10.1002/jgrd.50715.

——, S. Rudlosky, and W. Deierling, 2017: The evolution and structure of extreme optical lightning flashes. *J. Geophys. Res. Atmos.*, **122**, 333–349, https://doi.org/10.1002/2017JD026855.

Pitts, F. L., B. D. Fisher, V. Mazur, and R. A. Perala, 1988: Aircraft jolts from lightning bolts. *IEEE Spectrum*, **25** (7), 34–38, https://doi.org/10.1109/6.4573.

Qin, J., S. Celestin, and V. P. Pasko, 2012: Minimum charge moment change in positive and negative cloud to ground lightning discharges producing sprites. *Geophys. Res. Lett.*, **39**, L22801, https://doi.org/10.1029/2012GL053951.

Rakov, V. A., and M. A. Uman, 2007: *Lightning: Physics and Effects.* Cambridge University Press, 700 pp.

Rudlosky, S. D., S. J. Goodman, K. S. Virts, and E. C. Bruning, 2019: Initial Geostationary Lightning Mapper observations. *Geophys. Res. Lett.*, **46**, 1097–1104, https://doi.org/10.1029/2018GL081052.

Rutledge, S. A., and D. R. MacGorman, 1988: Cloud-to-ground lightning activity in the 10–11 June 1985 mesoscale convective system observed during the Oklahoma–Kansas PRESTORM project. *Mon. Wea. Rev.*, **116**, 1393–1408, https://doi.org/10.1175/1520-0493(1988)116<1393:CTGLAI>2.0.CO;2.

Schmit, T. J., P. Griffith, M. M. Gunshor, J. M. Daniels, S. J. Goodman, and W. J. Lebair, 2017: A closer look at the ABI on the GOES-R series. *Bull. Amer. Meteor. Soc.*, **98**, 681–698, https://doi.org/10.1175/BAMS-D-15-00230.1.

Stolzenburg, M., W. D. Rust, B. F. Smull, and T. C. Marshall, 1998: Electrical structure in thunderstorm convective regions: 1. Mesoscale convective systems. *J. Geophys. Res.*, **103**, 14059–14078, https://doi.org/10.1029/97JD03546.

Thomas, R. J., P. R. Krehbiel, W. Rison, S. J. Hunyady, W. P. Winn, T. Hamlin, and J. Harlin, 2004: Accuracy of the Lightning Mapping Array. *J. Geophys. Res.*, **109**, D14207, https://doi.org/10.1029/2004JD004549.

Turman, B. N., 1977: Detection of lightning superbolts. *J. Geophys. Res.*, **82**, 2566–2568, https://doi.org/10.1029/JC082i018p02566.

van der Velde, O., J. Montanya, S. Soula, N. Pineda, and J. Mlynarczyk, 2014: Bidirectional leader development in sprite-producing positive cloud-to-ground flashes: Origins and characteristics of positive and negative leaders. *J. Geophys. Res. Atmos.*, **119**, 12755–12779, https://doi.org/10.1002/2013JD021291.

Vonnegut, B., O. H. Vaughan Jr., M. Brook, and P. Krehbiel, 1985: Mesoscale observations of lightning from the space shuttle. *Bull. Amer. Meteor. Soc.*, **66**, 20–29, https://doi.org/10.1175/1520-0477(1985)066<0020:MOOLFS>2.0.CO;2.

Warner, T. A., K. L. Cummins, and R. E. Orville, 2012: Upward lightning observations from towers in Rapid City, South Dakota and comparison with National Lightning Detection Network data, 2004–2010. *J. Geophys. Res.*, **117**, D19109, https://doi.org/10.1029/2012JD018346.

——, J. H. Helsdon Jr., M. J. Bunkers, M. M. F. Saba, and R. E. Orville, 2013: UPLIGHTS: Upward Lightning Triggering Study. *Bull. Amer. Meteor. Soc.*, **94**, 631–635, https://doi.org/10.1175/BAMS-D-11-00252.1.

——, and Coauthors, 2018: Upward Lightning Triggering Study (UPLIGHTS): Project summary and initial Findings. *25th Int. Lightning Detection Conf./7th Int. Lightning Meteorology Conf.*, Ft. Lauderdale, FL, Vaisala, www.vaisala.com/sites/default/files/documents/Upward%20Lightning%20Triggering%20Study_T.A.%20Warner%20et.%20al.pdf.

Weiss, S. A., D. R. MacGorman, E. Bruning, and V. C. Chmielewski, 2018: Two methods for correcting range-dependent bias of Lightning Mapping Arrays. *J. Atmos. Oceanic Technol.*, **35**, 1273xn1282, https://doi.org/10.1175/JTECH-D-17-0213.1.

Williams, E. R., 1998: The positive charge reservoir for sprite-producing lightning. *J. Atmos. Sol.-Terr. Phys.*, **60**, 689–692, https://doi.org/10.1016/S1364-6826(98)00030-3.

——, and Coauthors, 2010: Ground-based detection of sprites and their parent lightning flashes over Africa during the 2006 AMMA Campaign. *Quart. J. Roy. Meteor. Soc.*, **136** (Suppl.), 257–271, https://doi.org/10.1002/qj.489.

Zipser, E. J., D. J. Cecil, C. Liu, S. W. Nesbitt, and D. P. Yorty, 2006: Where are the most intense thunderstorms on Earth? *Bull. Amer. Meteor. Soc.*, **87**, 1057–1072, https://doi.org/10.1175/BAMS-87-8-1057.